

Reconstitution of Rab11-FIP4 Expression Rescues Cellular Homeostasis in Cystinosis

Farhana Rahman^a, Jennifer L. Johnson^a, Mouad Ait Kbaich^a, Elsa Meneses-Salas^a, Aparna Shukla^a, Danni Chen^a, William B. Kiosses^b, Evripidis Gavathiotis^c, Ana Maria Cuervo^d, Stephanie Cherqui^e and Sergio D. Catz^a 

^aDepartment of Molecular and Cellular Biology, The Scripps Research Institute, La Jolla, California, USA; ^bDivision of Inflammation Biology, La Jolla Institute for Immunology, La Jolla, California, USA; ^cDepartment of Biochemistry, Albert Einstein College of Medicine, Bronx, New York, USA; ^dDepartment of Developmental and Molecular Biology, Albert Einstein College of Medicine, Bronx, New York, USA; ^eDepartment of Pediatrics, University of California San Diego, La Jolla, California, USA

ABSTRACT

Rab11 family interacting protein 4 (Rab11-FIP4) regulates endocytic trafficking. A possible role for Rab11-FIP4 in the regulation of lysosomal function has been proposed, but its precise function in the regulation of cellular homeostasis is unknown. By mRNA array and protein analysis, we found that Rab11-FIP4 is downregulated in the lysosomal storage disease cystinosis, which is caused by genetic defects in the lysosomal cystine transporter, cystinosin. Rescue of Rab11-FIP4 expression in *Ctns*^{-/-} fibroblasts re-established normal autophagosome levels and decreased LC3B-II expression in cystinotic cells. Furthermore, Rab11-FIP4 reconstitution increased the localization of the chaperone-mediated autophagy receptor LAMP2A at the lysosomal membrane. Treatment with genistein, a phytoestrogen that upregulates macroautophagy, or the CMA activator QX77 (CA77) restored Rab11-FIP4 expression levels in cystinotic cells supporting a cross-regulation between two independent autophagic mechanisms, lysosomal function and Rab11-FIP4. Improved cellular homeostasis in cystinotic cells rescued by Rab11-FIP4 expression correlated with decreased endoplasmic reticulum stress, an effect that was potentiated by Rab11 and partially blocked by expression of a dominant negative Rab11. Restoring Rab11-FIP4 expression in cystinotic proximal tubule cells increased the localization of the endocytic receptor megalin at the plasma membrane, suggesting that Rab11-FIP4 reconstitution has the potential to improve cellular homeostasis and function in cystinosis.

Abbreviations: (RAB11-FIP4): Rab11 family-interacting protein 4; (LRP2): Megalin; (PTCs): Proximal tubule cells; (CMA): Chaperone-mediated autophagy; (LAMP2A): Lysosomal-associated membrane protein type 2A; (LAMP1): Lysosomal-associated membrane protein type 1; (ER): Endoplasmic reticulum

ARTICLE HISTORY

Received 28 August 2024
Revised 25 September 2024
Accepted 26 September 2024

KEYWORDS


Lysosomal disease; trafficking; Rab GTPases; ER stress; autophagy; chaperone-mediated autophagy; Rab11; Rab11-FIP4; ATF4; Arf6

Introduction

Vesicular trafficking defects constitute central cellular anomalies of cystinosis, a lysosomal storage disorder caused by the accumulation of the amino acid cystine due to genetic defects in the *CTNS* gene, which encodes cystinosin, the lysosomal cystine transporter.^{1,2} Increased levels of intralysosomal cystine are associated with impaired intracellular trafficking and cell malfunction, which is especially manifested in the epithelial proximal tubule cells (PTCs) of the kidneys. Vesicular trafficking defects in cystinosis are both associated with and independent of the lysosomal overload.³⁻⁵ The observation that patients with full compliance with cysteamine treatment eventually progress to renal injury,⁶ supports that cystine accumulation is not the only cause of all the defects observed in cystinosis.^{6,7} The origin of vesicular trafficking defects in cystinosis are poorly understood.^{8,9} Among the previously described defects of vesicular

transport in this lysosomal-storage disorder (LSD), cystinotic proximal tubule cells present defective expression of the secretory GTPase Rab27a. Furthermore, upregulation of Rab27a-mediated vesicular trafficking mechanisms in cystinotic cells rescued the defective lysosomal transport phenotype and reduced lysosomal overload and ER stress.⁹ Defective trafficking mechanisms regulated by the Rab GTPase Rab7 have also been shown to affect cellular homeostasis in cystinosis. In particular, the subcellular localization of LAMP2A, a lysosomal receptor that regulates the rate of the transport of cytosolic protein cargoes for lysosomal degradation by a specialized form of autophagy named chaperone-mediated autophagy (CMA), is regulated by Rab7 and this regulation is defective in cystinosis.⁸ A similar role has been attributed to Rab11, although Rab7 and Rab11 are known to regulate LAMP2A trafficking from different subcellular compartments to lysosomes in cystinosis, and therefore their

CONTACT Sergio D. Catz  scatz@scripps.edu

 Supplemental data for this article can be accessed online at <https://doi.org/10.1080/10985549.2024.2410814>.

© 2024 The Author(s). Published with license by Taylor & Francis Group, LLC.

This is an Open Access article distributed under the terms of the Creative Commons Attribution-NonCommercial-NoDerivatives License (<http://creativecommons.org/licenses/by-nc-nd/4.0/>), which permits non-commercial re-use, distribution, and reproduction in any medium, provided the original work is properly cited, and is not altered, transformed, or built upon in any way. The terms on which this article has been published allow the posting of the Accepted Manuscript in a repository by the author(s) or with their consent.

functions appear to be complementary. While Rab GTPases are known to associate with specific subcellular compartments and regulate specific transport systems, their interactions with several molecular effectors define the specificity of these trafficking mechanisms; however, whether vesicular trafficking defects are associated with the malfunction of specific Rab effectors in cystinosis is currently unknown.

To further identify molecular effectors of vesicular trafficking that are defective in cystinosis, we performed comparative quantitative mRNA analysis of kidneys from wild-type and cystinotic mice and identified Rab11-FIP4 (Rab11 family interacting protein 4) to be downregulated in cystinosis. Although there are only a handful of publications about Rab11-FIP4, evidence suggests that Rab11-FIP4 is a Rab11 effector¹⁰ associated with the regulation of endosomal recycling,¹¹ proteasome localization,¹² progenitor differentiation,¹³ and cancer progression,¹⁴ although Rab11-independent functions have also been described for Rab11-FIP4.¹⁵

Here, we show that Rab11-FIP4 is downregulated in cystinosis and that reconstitution of the expression of this Rab11

effector improves cellular homeostasis and increases the distribution of megalin at the plasma membrane in cystinotic PTCs. Our data support that vesicular transport defects are associated with both homeostatic and cellular-specific defects in this disease and the inclusion of Rab11-FIP4 on the list of possible therapeutic targets for this lysosomal disease.

Results

Rab11-FIP4 is downregulated in cystinotic cells

Rab GTPase downregulation is associated with vesicular trafficking defects in cystinosis.⁹ In particular, decreased Rab7 and Rab11 expression is linked to the defective trafficking of LAMP2A, impaired CMA, and defective megalin localization but the molecular pathways regulated by these GTPases and the Rab effectors associated with these defects in cystinosis are yet to be elucidated. Using mRNA analysis of cystinotic kidneys, we identified the Rab11 effector *Rab11-fip4* to be downregulated in kidneys from *Ctns*^{-/-} mice (Figure 1A

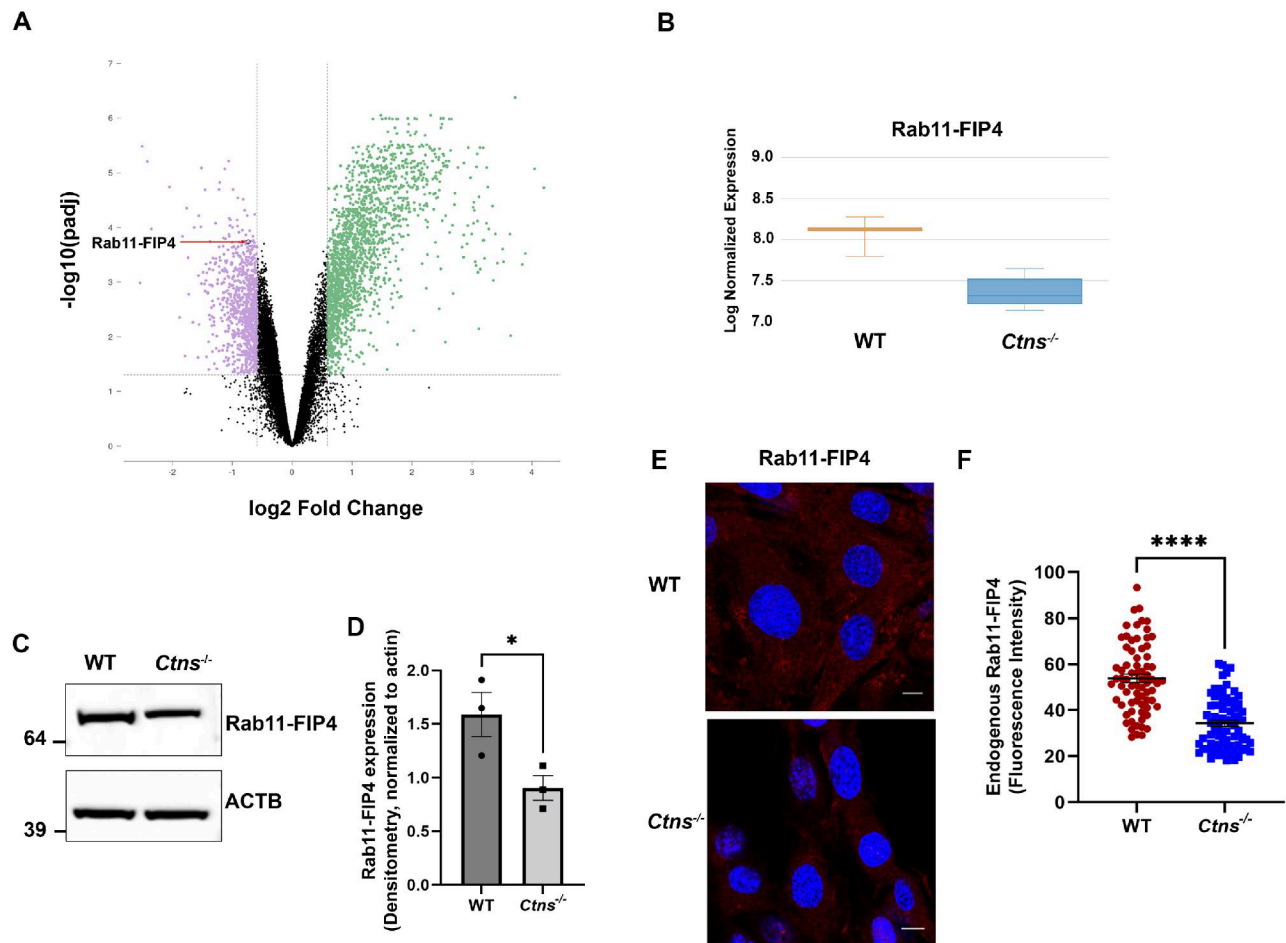


Figure 1. Rab11-FIP4 is downregulated in cystinotic cells. (A and B) Volcano plot and box representations of differential gene expression analysis in kidneys from WT and *Ctns*^{-/-} mice. The differentially expressed genes (DEGs) identified in six wild-type and six *Ctns*^{-/-} kidney samples are presented in ref¹⁶. (C) Expression of Rab11-FIP4 in WT and *Ctns*^{-/-} fibroblasts analyzed by Western blot. (D) Quantification of Rab11-FIP4 expression (normalized to actin, ACTB) from three independent experiments. Mean \pm SEM * P < 0.05, unpaired Student's t test. (E) Immunofluorescence analysis of endogenous Rab11-FIP4 expression in wild-type and *Ctns*^{-/-} MEFs. Scale bar, 10 μ m. (F) Quantification of Rab11-FIP4 fluorescence intensity (RFU). Each symbol represents the average fluorescence intensity of the cells per field. A total of 25 fields and >70 cells were quantified for WT and *Ctns*^{-/-} samples, respectively, in three independent experiments. Mean \pm SEM, **** P < 0.0001, unpaired Student's t test.

and B).¹⁶ The downregulation of endogenous Rab11-FIP4 protein in cystinotic fibroblast was confirmed by immunoblotting (Figure 1C). Thus, quantitative analysis showed that Rab11-FIP4 expression is significantly decreased in cystinotic cells compared to wild-type cells (Figure 1D). As control, cystinotic cells were routinely checked for lysosomal overload using mass spectrometry analysis of accumulated cystine as described.³ The decreased expression of Rab11-FIP4 was confirmed by immunofluorescence analysis of the endogenous protein (Figure 1E and F).

RAB11-FIP4 rescues LAMP2A localization at lysosomes in cystinosis

Previous studies from our group showed that CMA defects are central to cystinosis disease. In particular, downregulation and mislocalization of LAMP2A, the only known specific lysosomal receptor that targets proteins for degradation in CMA, is mislocated at Rab11+ carrier vesicles in cystinosis.³ In addition, our previous studies showed that the recycling endosome-associated Rab GTPase Rab11 is downregulated in cystinosis and that Rab11 overexpression rescues some of the vesicular trafficking defective phenotypes in cystinotic cells,⁸ including that of LAMP2A, although how Rab11 mediates this process is currently unknown. Here, we raised the question of whether Rab11-FIP4 reconstitution is sufficient to increase the lysosomal location of LAMP2A. To this end, we first studied the lysosomal localization of endogenous LAMP2A related to the endolysosomal marker LAMP1. As expected, LAMP2A localization at LAMP1+ endolysosomes was decreased in *Ctns*^{-/-} cells (Figure 2A and B). However, *Ctns*^{-/-} cells with reconstituted Rab11-FIP4 expression, showed Rab11-FIP4 partial localization at the endolysosomal compartment (magenta arrowheads in Figure 2A, magnified) and re-localization of the CMA receptor LAMP2A to the lysosomal compartment, which was confirmed by quantitative analysis of the colocalization of LAMP2A with the lysosomal marker LAMP1 (Figure 2B). Because LAMP2A trafficking is regulated by the small GTPases Rab11, which is also downregulated in cystinosis, we next analyzed whether Rab11 expression rescues the decreased expression of Rab11-FIP4 in cystinotic cells. In these experiments, we used human kidney cells in which CTNS expression was downregulated using siRNA (CTNS-KD, Supplementary Figure S1). We show that endogenous Rab11-FIP4 is downregulated in CTNS-KD cells (Figure 2C and D). We also show that exogenous Rab11 expression does not rescue the decreased expression of endogenous Rab11-FIP4 (Figure 2C and D). Furthermore, the expression of Rab7 and Rab11, previously shown to regulate LAMP2A trafficking in cystinosis,⁸ were not increased in CTNS-KD cells rescued with Rab11-FIP4 CTNS-KD (Supplementary Figure S2), suggesting that the rescue of the LAMP2A mislocalization phenotype caused by Rab11-FIP4 is not mediated by the upregulation of these GTPases.

Rab11-FIP4 decreases autophagosome accumulation in cystinosis

Impaired vesicular trafficking has a negative impact on cell homeostasis mechanisms, including autophagic pathways, and cystinosis cells are characterized by autophagy alterations, including autophagosome accumulation.³ Here, to determine whether reconstitution of Rab11-FIP4 expression rescues the vesicular transport-associated autophagic pathways defects observed in cystinotic cells, we next analyzed LC3 turnover comparatively in wild-type, *Ctns*^{-/-} and Rab11-FIP4 reconstituted *Ctns*^{-/-} cells. Cystinotic cells are characterized by increased basal autophagosome accumulation but normal SQSTM1 clearance.^{3,17} We found that Rab11-FIP4 reconstituted *Ctns*^{-/-} cells present reduced autophagosome accumulation as compared to parent *Ctns*^{-/-} cells (Figure 3A and B). Rab11-FIP4 reconstitution also decreased autophagosome accumulation under starvation conditions in cystinosis (Figure 3A and B).

Because upregulation of both macroautophagy and CMA have a positive impact on lysosomal storage disorders and, in particular, on cystinosis, we next analyzed the effect of pharmacological manipulation of autophagic processes on Rab11-FIP4 expression. We found that genistein (5,7-dihydroxy-3-(4-hydroxyphenyl)-4H-1-benzopyran-4-one), a phytoestrogen that upregulates macroautophagy through activation of the master regulator of lysosomal biosynthesis, TFEB,¹⁸ restores Rab11-FIP4 expression levels in cystinotic cells (Figure 4A and B). Furthermore, a significant increase in Rab11-FIP4 expression was also observed in *Ctns*^{-/-} cells after treatment with the CMA activator QX77 (CA77) (Figure 4A and B), which increases survival in cystinosis cells exposed to oxidative stress,⁸ and whose analogue, CA77.1, was recently shown to ameliorate proteotoxicity and neurodegeneration.¹⁹ The results presented here suggest a crosstalk regulation between two independent autophagic homeostasis mechanisms and the trafficking molecule Rab11-FIP4. Our data also indicate that Rab11-FIP4, like other lysosomal and autophagy regulatory factors, is likely a transcriptional target of TFEB.

RAB11-FIP4 decreases ER stress in cystinosis

Impaired vesicular trafficking in cystinosis is associated with increased endoplasmic reticulum (ER) stress and susceptibility to oxidative stress.^{3,9} To evaluate whether the rescue of Rab11-FIP4 expression has a positive impact on cellular homeostasis in cystinosis, we analyzed the effect of Rab11-FIP4 reconstitution on the expression levels of the UPR target protein GRP78, an ER stress marker upregulated in *Ctns*^{-/-} cells.⁹ Quantitative immunofluorescence analysis showed that Rab11-FIP4 reconstitution induces a significant decrease in the fluorescence intensity of endogenous GRP78 in *Ctns*^{-/-} fibroblasts compared to both mock-transfected control cystinotic cells (Figure 5A and B) and adjacent nonexpressing GFP-Rab11-FIP4 cystinotic cells, which served as internal control (Figure 5A, bottom panel, magenta arrow). The ER stress rescued phenotype exerted by Rab11-FIP4 in *Ctns*^{-/-} cells was further confirmed by the analysis of the expression of KDEL-reactive GRP78 expression by immunoblotting (Figure

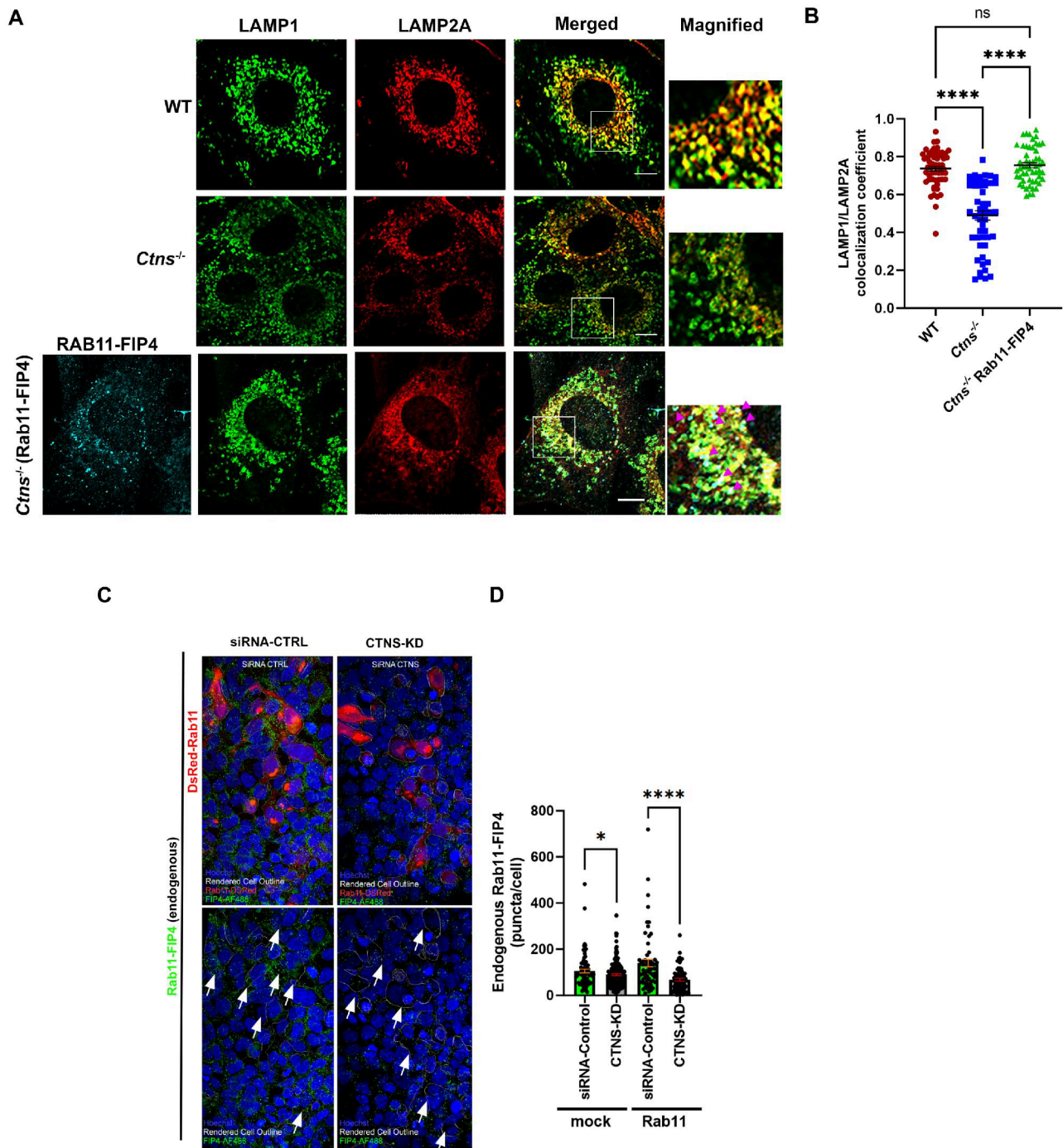


Figure 2. (A) Immunofluorescence analysis of endogenous LAMP1 (pseudo-colored green) and LAMP2A (red) localization in WT, *Ctns*^{-/-} cells and GFP-Rab11-FIP4 (pseudo-colored cyan) expressing *Ctns*^{-/-} cells. Scale bar, 10 μ m. Magenta arrowheads in magnified image point to areas of colocalization between Rab11-FIP4, LAMP1, and LAMP2A. (B) Quantification of the colocalization of LAMP2A and LAMP1 shown in A. A total of 20 fields and 57, 53 and 54 cells were quantified for WT, *Ctns*^{-/-} and Rab11-FIP4 reconstituted *Ctns*^{-/-} cells, respectively, in 4 independent experiments. Mean \pm SEM, **** P < 0.0001; ns, not significant. One way ANOVA, Tukey's multiple comparison test. (C and D) Immunofluorescence analysis of the effect of Rab11 expression on the endogenous levels of Rab11-FIP4 in CTNS down-regulated cells (siRNA-CTNS, CTNS-KD) or control cells (siRNA-CTRL). (C) Where indicated, the cells were transfected for the expression of DsRed-Rab11a (Upper panel, red). In the bottom panels, outlines and arrows indicate the cells expressing DsRed-Rab11a in the top panel, showing that exogenous Rab11a expression (arrows) do not rescue the decreased expression of Rab11-FIP4 in CTNS-KD cells compared to untransfected CTNS-KD cells in the same panel. (D) Quantification of Rab11-FIP4 fluorescence intensity. Mean \pm SEM, * P < 0.05; **** P < 0.001.

5C and D), thus supporting that upregulation of the Rab11-FIP4-associated vesicular trafficking mechanisms decreases ER stress in cystinosis. Next, to test whether Rab11-FIP4 operates through Rab11 in rescuing the increased ER stress phenotype, we analyzed the effect of Rab11-FIP4 reconstitution in cells that express either wild-type or dominant-negative (DN) Rab11. Here, we show that expression of DN-Rab11a

attenuates the rescue mediated by Rab11-FIP4 while co-expression with WT Rab11 potentiates it (Figure 5E and F). However, DN-Rab11 did not completely abolish the rescue mediated by Rab11-FIP4, suggesting that Rab11-independent mechanism may operate in this process.

Defective cellular homeostasis, impaired ER stress and increased oxidative stress are all characteristics of cystinotic

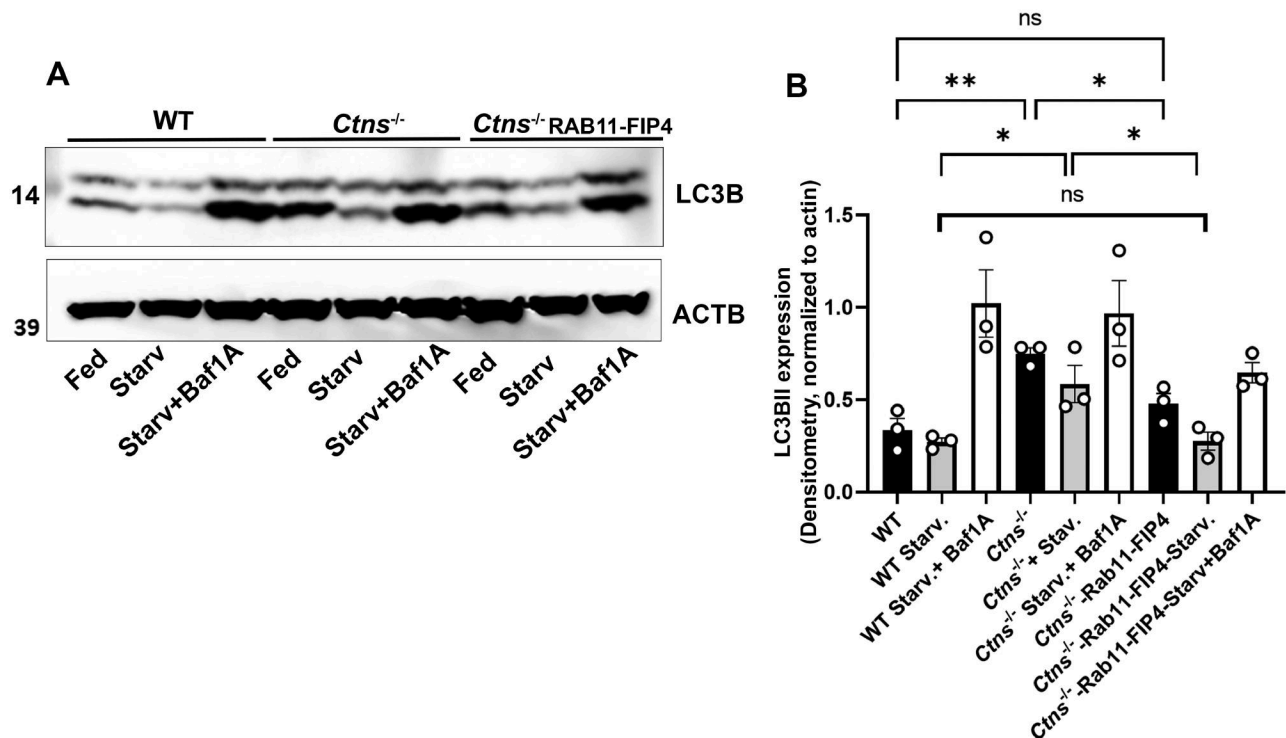


Figure 3. Reconstitution of Rab11-FIP4 decreases autophagosome accumulation in cystinosis. (A) WT, *Ctns*^{-/-} and GFP-Rab11-FIP4 fibroblasts under resting conditions were either fed or underwent serum starvation for 5 h (starv), in the presence or absence of 100 nM bafilomycin 1A (Baf1A). Endogenous LC3B-II expression was analyzed by Western blot. (B) Quantification of LC3B-II expression (normalized to actin, ACTB) from three independent experiments. **P* < 0.05; ***P* < 0.01; ns, not significant. One-way ANOVA, Tukey's multiple comparison test for each condition.

cells.¹⁶ Because oxidative stress and persistent ATF4 activation are associated with impaired CMA and decreased survival, we next study the role of Rab11-FIP4 on ATF4 localization and ROS production in cystinosis. First, using enhanced-resolution microscopy (Airyscan), we analyzed ATF4 nuclear localization as a readout for activation of the PERK arm of the UPR. Nuclear localization of endogenous ATF4, scarcely detected in wild-type cells, was markedly and significantly increased in siRNA-CTNS-KD cells. Furthermore, ATF4 nuclear localization in siRNA-CTNS-KD cells was significantly decreased by the rescue of Rab11-FIP4 expression (Figure 6A and B), validating the results for Grp78 and supporting that upregulation of vesicular trafficking decreases ER stress. Rab11-FIP4 has been described to operate as an effector for the GTPase ARF6.²⁰ Next, we studied whether Rab11-FIP4 mediated rescue of ER stress in cystinosis requires ARF6. To this end, we treated WT and CTNS-KD cells expressing GFP-Rab11-FIP4, with the selective ARF6 inhibitor NAV2729.²¹ Here, we show that the rescue of the increased-ATF4-nuclear-localization phenotype by Rab11-FIP4 in cystinotic cells is prevented by treatment with the ARF6 inhibitor (Figure 6A and B). Our data indicate that Rab11-FIP4 requires ARF6 to rescue the increased nuclear localization of ATF4 in cystinosis.

We previously showed that *Ctns*^{-/-} cells present increased endogenous levels of reactive oxygen species. Next, we analyzed whether the reconstitution of Rab11-FIP4 expression decreases the dysregulated oxidative stress in cystinosis. To this end, we analyzed reactive oxygen species using the ROS-sensitive fluorescent probe CellROX™. We show that reconstitution of Rab11-FIP4 expression significantly decreases oxidative stress in these *Ctns*^{-/-} cells (Figure 6C and D). Altogether, our data suggest that the upregulation of

Rab11-FIP4 expression has a beneficial impact on cellular homeostasis in cystinosis.

Rab11-FIP4 contributes to the rescue of the distribution of megalin at the plasma membrane in cystinotic proximal tubular cells

Proximal tubular cell (PTC) dedifferentiation including the loss of the apical receptor megalin (LRP2) contributes to the development of Fanconi syndrome in cystinosis.²² We showed that *CTNS*-KO human PTCs are characterized by increased ER stress, and impaired megalin trafficking.^{8,17} Here, we show that similar to *Ctns*^{-/-} fibroblasts, Rab11-FIP4 expression is downregulated in *CTNS*-KO PTCs (Figure 7A and B). To study whether Rab11-FIP4 reconstitution directly impacts megalin localization in PTC function, we next analyzed the localization of the receptor megalin in wild-type, *CTNS*-KO cells and in *CTNS*-KO PTCs with the reconstituted expression of Rab11-FIP4. Importantly, Rab11-FIP4 significantly increased the plasma membrane localization of megalin in cystinotic PTCs (Figure 7C and D), suggesting that the upregulation of the endocytic trafficking regulator has the potential to improve tubular cell function in cystinosis.

Discussion

Several lines of evidence point to vesicular trafficking as a central defective mechanism in the lysosomal disease cystinosis. Cystinosis, a transmembrane cystine transporter with lysosomal localization, has been proposed to mediate

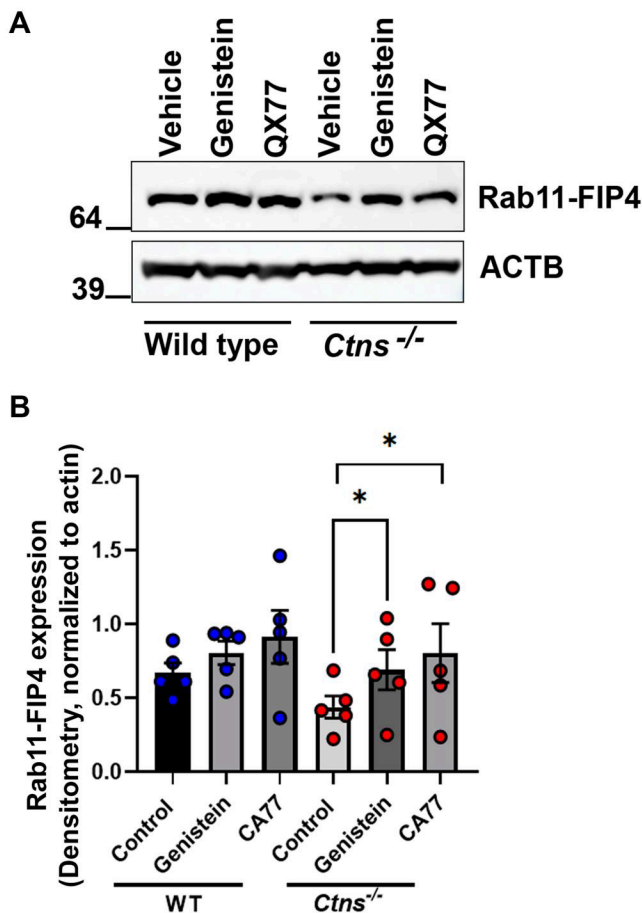


Figure 4. Increased Rab11-FIP4 expression by macroautophagy and CMA activation. (A) WT and *Ctns*^{-/-} fibroblasts were treated with DMSO (Vehicle), Genistein or QX77 (CA77) for 48 h, and Rab11-FIP4 expression levels were analyzed by Western blot. (B) Quantitative analysis of Rab11-FIP4 expression levels. The expression level of Rab11-FIP4 was normalized to actin in each sample. n = 5. *P < 0.05, paired Student's *t* test.

trafficking pathways.³ However, independent observations of downregulated or dysfunctional trafficking molecules described a picture in which several transport systems appear independently affected by the impairment of trafficking pathways in cystinotic cells. Rab GTPases and their effector molecules define the identity, function, and fate of specific membrane compartments. Three of these GTPases, Rab27a,⁹ Rab11,³ and Rab7,⁸ in chronological order of their reported involvement in cystinosis, have been associated with specific defective pathways in this LSD. However, none of the molecular effectors previously associated with these GTPases have been identified as defective in cystinosis so far. Because Rab GTPases show promiscuity related to their binding to specific effectors and because the expression of these effectors is generally more restricted than that of their counterpart GTPases, the discovery made in this work that the Rab11 atypical effector Rab11-FIP4 is downregulated in cystinotic cells poses important biological significance.

Rab11 has been largely associated with its role in the recycling of endosomes to redirect internalized proteins and cargoes toward the plasma membrane but also regulates other cellular functions including cytokinesis, ciliogenesis, receptor recycling, and autophagy. Rab11 function is regulated by a

family of Rab effectors with low homology which includes Rip11, Rab11-FIP1, Rab11-FIP2, Rab11-FIP3, RCP, Rab11-FIP4, and Rab11-FIP5.^{23–28} The interaction of Rab11 with Munc13-4, a Rab effector not included in this family, has also been demonstrated by our group.²⁹ Based on the lack of phospholipid-binding C2 domains and the presence of EF-hand domains, FIP3 and FIP4 are classified as class II FIPs. Similar to other FIP family members, Rab11-FIP4 contains a coiled-coil dimerization domain at the C-terminus of the protein which was proposed to mediate binding to two Rab11 molecules.²⁴ Although this domain was demonstrated to be sufficient to localize Rab11-FIP4 to endosomal compartments and its expression causes the dispersal of endosomes towards the cell periphery, it did not inhibit transferrin recycling¹⁰ suggesting that Rab11-FIP4 may not operate as a recycling endosome regulator. In this work, we observed that Rab11-FIP4 rescues the subcellular localization of LAMP2A increasing its distribution at the lysosomal membrane. This observation, together with our previous data showing that Rab11 regulates the direct delivery of LAMP2A to the lysosome but not to the plasma membrane,⁸ supports the view that Rab11-FIP4 contributes to the delivery of LAMP2A to lysosomes independently of endosome recycling or the so-called indirect pathway. How Rab11-FIP4 may regulate this process is currently unknown, but one possibility is that similar to other FIPs,²⁵ Rab11-FIP4 may bind to and regulate motor proteins. We recently showed that, like Rab11-FIP4, DYNC1L2 is downregulated in cystinosis, and its reconstitution not only rescues LAMP2A localization, but also increases CMA activity.¹⁶ The DYNC1L2 paralog DYNC1L1 was recently shown to form a tripartite complex with Rab11 and Rab11-FIP3 in A431 cells,³⁰ thus raising the question of whether Rab11-FIP4 also bridges Rab11+ vesicles to the retrograde transport by associating with a cytoplasmic dynein. Supporting this, using mass spectrometry analysis of proteins that were pulldown with Rab11-FIP4 we identified DYNC1L2 as a Rab11-FIP4 interactor (Supplementary data, Table 1), suggesting that Rab11-FIP4 and DYNC1L2 regulate a common mechanism of LAMP2A trafficking. Furthermore, ARF6, a small GTPase previously shown to interact with Rab11-FIP4, also appears to be important for the homeostatic rescue mediated by Rab11-FIP4 as the process is inhibited by the specific allosteric ARF6 inhibitor NAV2729. Finally, we found that Rab11-FIP4 interacts with Rab34, a Rab GTPase recently found to regulate lysosomal positioning and autophagy together with dynein and RILP, in an Arl8b-dependent manner.³¹ Our data thus highlight possible divergent mechanisms mediated by Rab11-FIP4 interactors in the regulation of CMA and macroautophagy.

Besides the association between Rab11-FIP4 and LAMP2A trafficking, we found that Rab11-FIP4 regulates trafficking mechanisms in cystinosis that are independent of the CMA pathway. In particular, Rab11-FIP4 reconstitution significantly rescued the defective macroautophagy phenotype in cystinotic cells by reducing the accumulated autophagosomes. Prior research associates Rab11 with the initiation or the maturation of autophagosomes and the regulation of macroautophagy. For instance, overexpression of dominant-negative Rab11 has been shown to decrease LC3 lipidation although overexpression of wild-type or constitutively active Rab11 has no or a very slight effect on

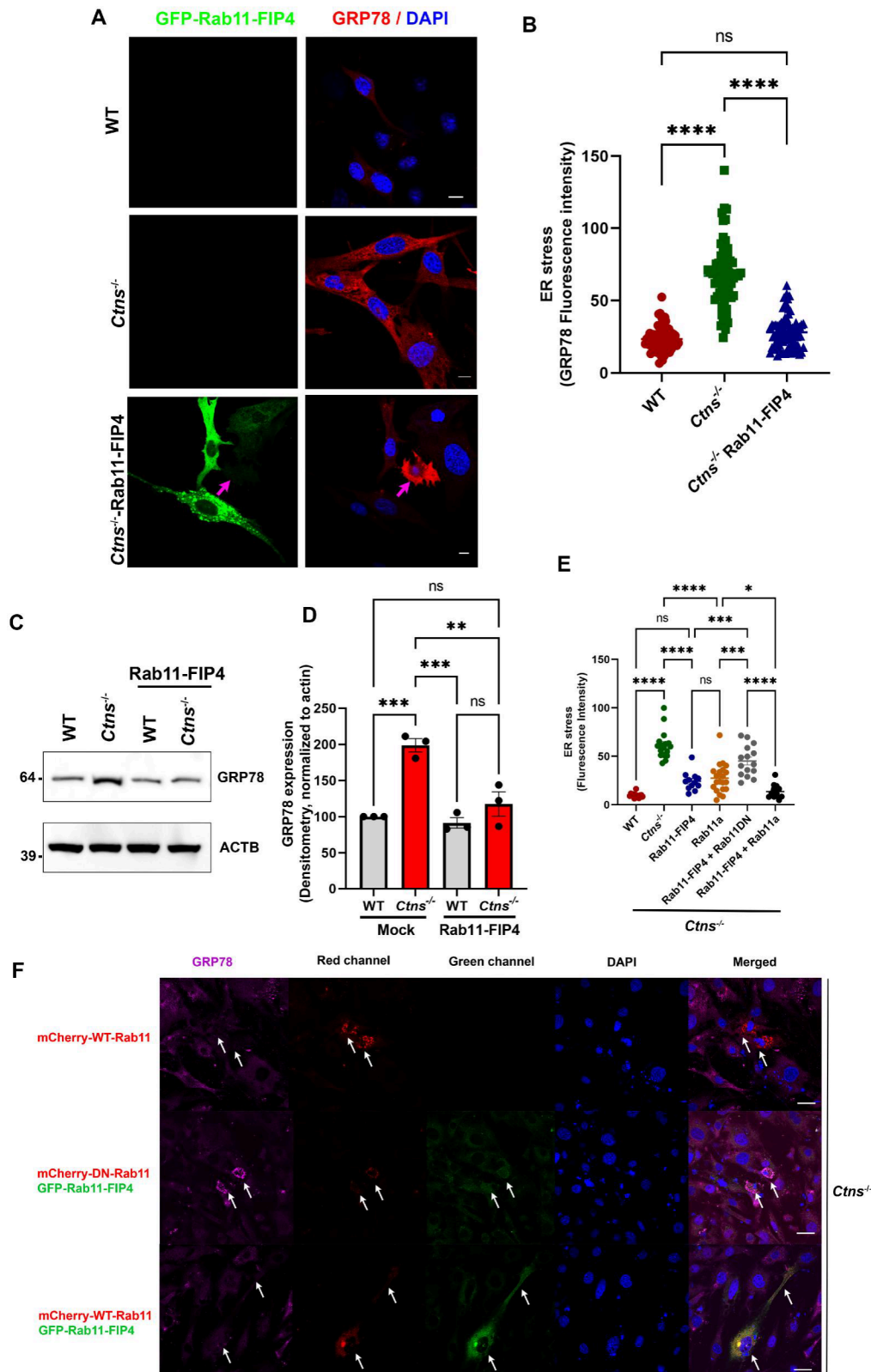


Figure 5. Rescue of Rab11-FIP4 expression reduces ER stress in *Ctns*^{-/-} cells. (A) The expression level of the established UPR target gene GRP78, which is induced during conditions of ER stress, was analyzed in wild-type (WT), *Ctns*^{-/-} cells, and *Ctns*^{-/-} cells expressing GFP-Rab11-FIP4, by immunofluorescence analysis, using a mouse monoclonal anti-KDEL antibody. Scale bar, 10 μ m. The magenta arrow points to untransfected cells that serve as internal control. (B) Quantification of GRP78 fluorescence intensity. Each symbol represents the average fluorescence intensity of the cells per field. A total of 25 fields and 71, 74, and 81 cells were quantified for WT, *Ctns*^{-/-} and *Ctns*^{-/-}-GFP-Rab11-FIP4 cells, respectively, in three independent experiments. (C) Western blot analysis of GRP78 expression in wild-type (WT), *Ctns*^{-/-}, and GFP-*Ctns*^{-/-}-Rab11-FIP4 fibroblasts. (D) Quantification of GRP78 expression levels (normalized to actin, ACTB) from three independent experiments. * $p < 0.05$; ** $p < 0.01$; *** $p < 0.001$; ns, not significant. (E) The quantification of GRP78 fluorescence intensity in WT, *Ctns*^{-/-} and *Ctns*^{-/-} cells expressing either GFP-Rab11-FIP4, Rab11a, both GFP-Rab11-FIP4 and dominant negative (DN) Rab11a or both GFP-Rab11-FIP4 and WT Rab11a. (F) Representative images of the experiments quantified in E. The arrows indicate transfected cells with the respective plasmids. * $p < 0.05$; *** $p < 0.001$; **** $p < 0.0001$, ns, not significant. (B, D, and E) One-way ANOVA, Tukey's multiple comparison test.

macroautophagy, respectively.³² Although Rab11 was not detected in LC3+ tubular structures, it regulates the perinuclear localization of Atg16L1-positive recycling endosomes to facilitate LC3 recruitment.³³ Similarly, although Rab11-FIP3 did not affect LC3-II formation, it induced tubulation of endosomal structures possibly associated with Atg13 recruitment.³² Other studies have shown that in K562 cells, Rab11 colocalizes with LC3-positive structures and suggested that it regulates autophagosome maturation,³⁴ and/or amphisome formation.³⁵ Our findings that Rab11-FIP4 reconstitution decreases the accumulation of lipidated LC3 under fed and starvation conditions in cystinosis highlight a possible role for this class II FIP Rab effector in macroautophagy regulation under conditions of lysosomal overload.

While vesicular dynamics and directional movement control the fate of an organelle and its interacting organelles, for example, through membrane contact sites,³⁶ defects in vesicular transport are associated with altered homeostatic mechanisms that lead to cellular dysfunction including stress of the ER. We previously showed that reconstitution of the dynein subunit DYNC1L2 decreases ER stress in cystinosis in a LAMP2A-dependent manner. Here, we show that the upregulation of Rab11-FIP4 has a similar effect. Reconstitution of the Rab effector not only decreased the level of accumulated HSPA5 (Grp78) in cystinotic cells but also decreased the nuclear accumulation of ATF4, a transcription factor associated with the upregulation of CHOP and the initiation of apoptotic pathways. The identification of DYNC1L2 as a Rab11-FIP4 interactor may indicate that these two trafficking modulators share a common pathway in the regulation of ER stress.

In this work, Rab11-FIP4 upregulation is shown to improve cellular homeostasis in cystinosis at many levels. For instance, the correction of LAMP2A lysosomal localization and decreased autophagosome accumulation was accompanied by a significant decrease in the levels of endoplasmic reticulum stress, a hallmark of cystinotic cells, supporting the idea that the reconstitution of Rab11-FIP4-dependent vesicular mechanisms has a direct and positive impact on cellular function and homeostasis in cystinosis thus highlighting the concept that the upregulation of vesicular trafficking leads to an improvement in organelle function and cellular homeostasis. In human PTCs with cystinosis deficiency, Rab11-FIP4 upregulation increased the plasma membrane localization of megalin, an important endocytic receptor whose downregulation is a hallmark of the disease as it is directly linked to impaired tubule function and Fanconi syndrome.³⁷ Our data suggest that Rab11-FIP4 reconstitution upregulates several independent vesicular trafficking pathways that ultimately lead to the improvement of cellular function thus highlighting Rab11-FIP4 as the first Rab effector whose expression has direct implications on disease development and thus its potential as a new therapeutic target for cystinosis.

Experimental procedures

Animal models and cell lines

All animal studies were performed in compliance with the United States Department of Health and Human Services Guide for the Care and Use of Laboratory Animals. All studies

were conducted according to National Institutes of Health and institutional guidelines and with the approval of the animal review boards at The Scripps Research Institute and University of California, San Diego. All animal protocols and procedures were approved by the ethic committee, Institutional Animal Care and Use Committee, under protocol number: 08-0078-6. The C57BL/6 *Ctns*^{-/-} mice were described before.³⁸ Neonatal mouse embryonic fibroblasts from *Ctns*^{-/-} and wild-type mice were prepared by standard procedures.³ The cystinosin knockout human proximal tubule cell line was generated using CRISPR/Cas9 and described previously.¹⁷ Neonatal murine fibroblasts were maintained in Dulbecco's modified Eagle's medium supplemented with 10% FBS (Corning Cellgro) and penicillin/streptomycin/glutamine (Life Technologies). The human kidney epithelial-like cell line 293FT was acquired from ATCC. For cystinosin downregulation, the cells were transfected using siRNA (Dharmacon, pool) and DharmaFECT Transfection Reagent. The cells were recovered for 24 h and subsequently transfected with the indicated constructs for the expression of GFP-Rab11-FIP4 and/or DsRED-Rab11 expression.

Gene expression

Animals were housed and studied according to NIH Guidelines for the Care and Use of Laboratory Animals. Sixteen months old C57BL/6 wild-type (n = 6) and *Ctns*^{-/-} (n = 6) mice were euthanized and the kidneys immediately removed and stored at -80°C in RNA Later (Life Technologies). Tissues were subsequently ground using Precellys 24 (Bertin Technologies) and RNA was isolated using the Qiagen AllPrep DNA/RNA Mini kit (Qiagen). The RNA was run on a Bioanalyzer (Agilent) for quantification and quality assessment. The Ambion WT Expression Kit was used to generate double-stranded biotinylated cDNA and the Affymetrix HT WT Terminal Labeling Kit was used to prepare the cDNA for hybridization to Affymetrix GeneChip Mouse Gene 1.1 ST arrays (Affymetrix). The double-stranded biotinylated cDNA from each tissue for each mouse was run on individual Affymetrix GeneChip. The data was collected as CEL files and quality control analysis performed with Affymetrix Expression Console. Normalized signal intensities were generated with Robust Multichip Average (RMA) which employs a background adjustment and quantile normalization strategy.³⁹ Genes without an average log₂ transformed signal >6 in either the wild-type or *Ctns*^{-/-} group were removed from further analysis. Class comparisons of variance by two-way *t* tests for two sample comparisons (*P* < 0.001) were performed using BRB-ArrayTools (<http://linus.nci.nih.gov/BRB-ArrayTools.html>) to identify the set of significantly differentially expressed genes between wild-type and *Ctns*^{-/-} mice in each tissue. Pathway analyses were performed, and images generated using ROSALINDTM, OnRamp Bioinformatics.

Constructs, transfections, and transductions

The expression vector pEZ-M98 expressing EGFP-Rab11-FIP4 was obtained from GeneCopoeia and was analyzed by

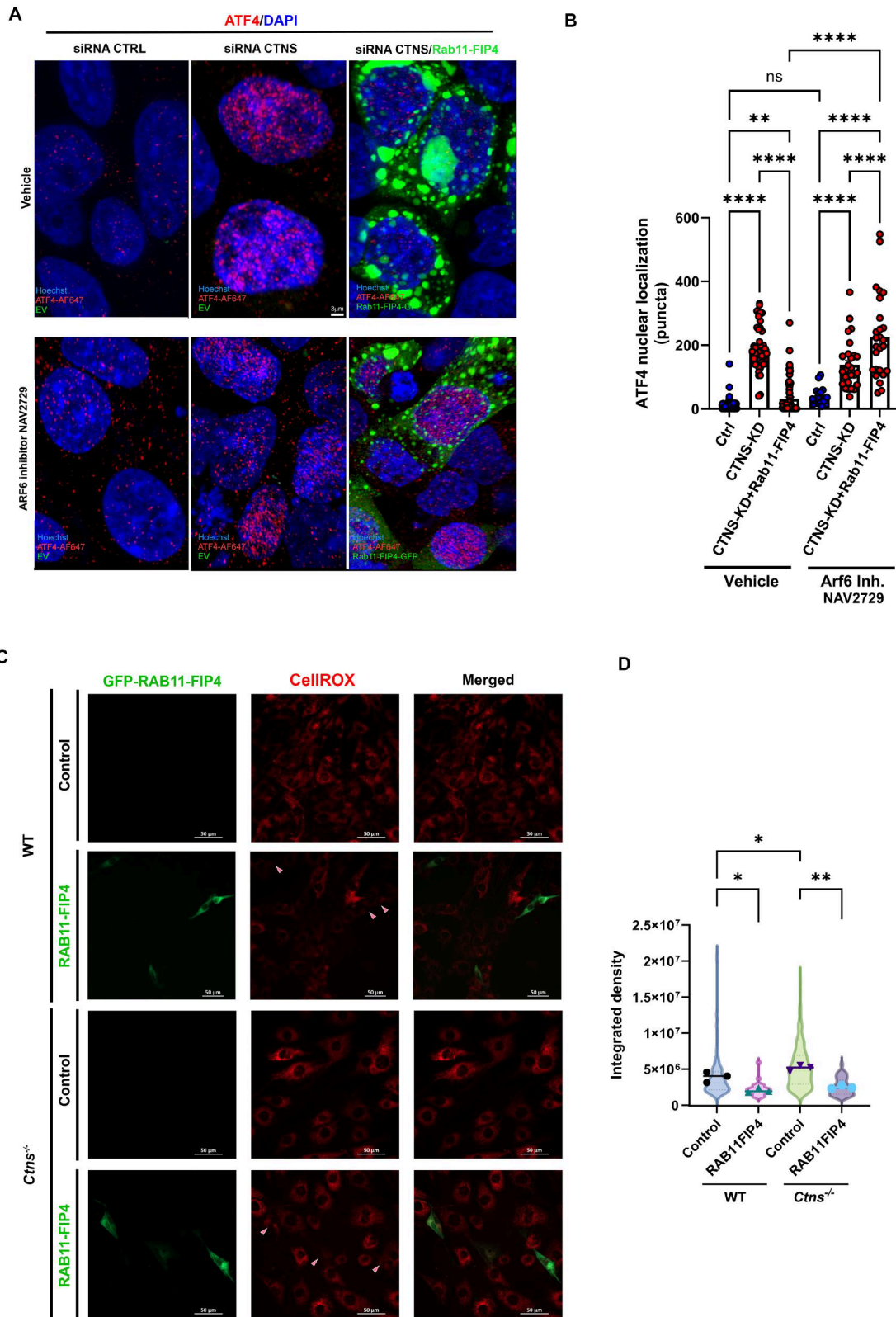


Figure 6. Rab11-FIP4 decreases ATF4 nuclear localization in an Arf6-dependent manner. (A and B) Immunofluorescence and enhanced-resolution microscopy analysis of endogenous ATF4 (Red) in CTNS-downregulated cells (siRNA-CTNS) or control cells (siRNA CTRL). Where indicated, the cells were transfected for the expression of GFP-Rab11-FIP4 or mock transfected (EV). The cells were treated with the ARF6 inhibitor NAV2729 or Vehicle (DMSO). (A) Representative enhanced-resolution (Airyscan) microscopy images. (B) Quantitative analysis of ATF4 nuclear localization. Each symbol represents an independent cell. Mean \pm SEM. $**P < 0.01$ and $****P < 0.0001$. One-way ANOVA, Tukey's multiple comparison test. (C and D) Rab11-FIP4 reconstitution decreases oxidative stress in cystinosis. Intracellular reactive oxygen species (ROS) accumulation in WT, *Ctns*^{-/-} and Rab11-FIP4-reconstituted *Ctns*^{-/-} living cells was studied by fluorescence microscopy analysis using the cell-permeable probe CelliROX (5 μ M). (C) Representative images. The arrowheads indicate *Ctns*^{-/-} cells expressing Rab11-FIP4-GFP and their respective CelliROX levels. (D) Quantitative analysis of the fluorescence intensity (CelliROX) in cells expressing Rab11-FIP4 and cells not expressing the chimera in the same field. Each dot in the superplot represents the average of an independent experiment. $n = 3$. Mean \pm SEM. $*P < 0.05$ $**P < 0.01$.

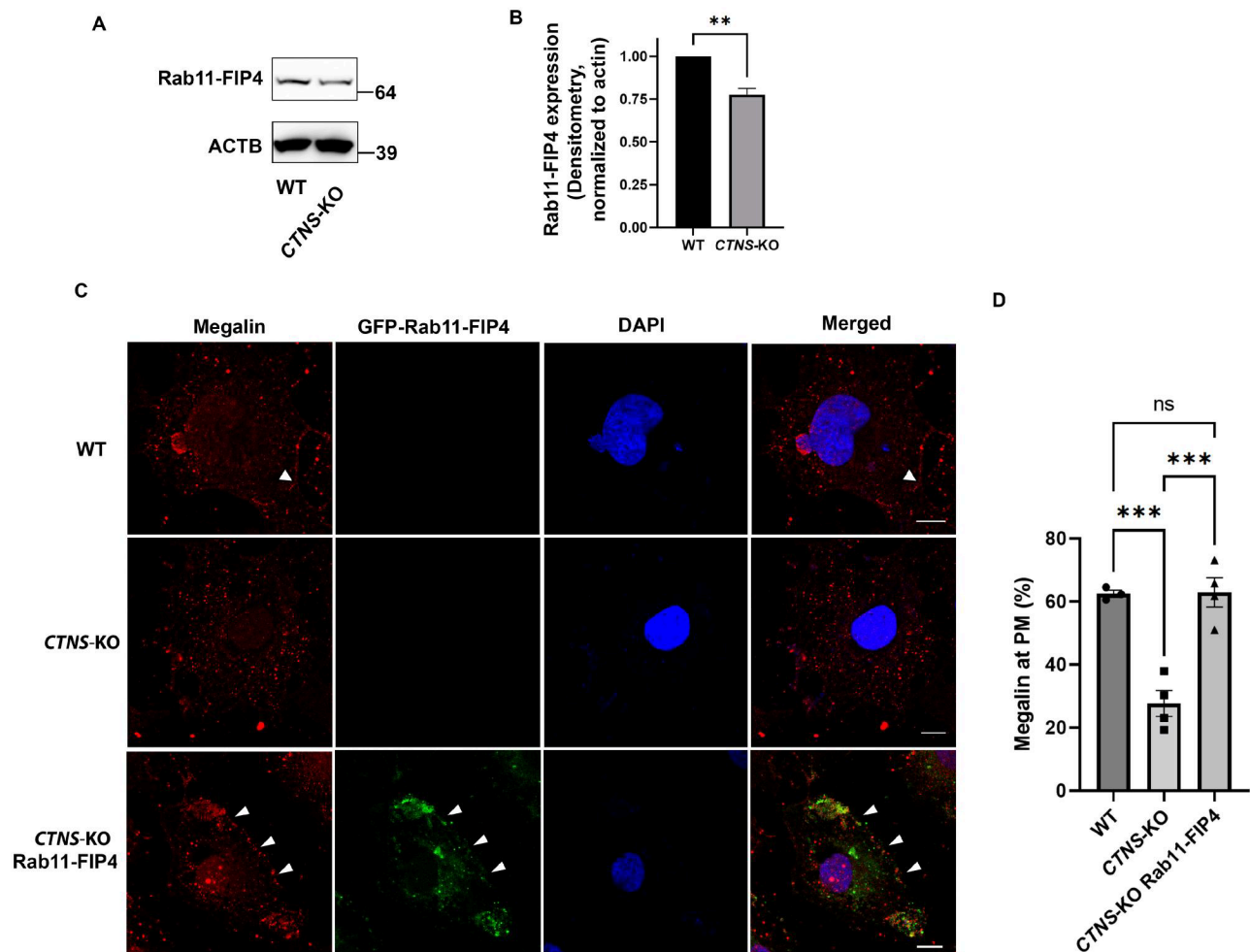


Figure 7. Rab11-FIP4 increases Megalin (LRP2) localization at the plasma membrane in cystinotic proximal tubule cells. (A) Expression of Rab11-FIP4 in WT and *CTNS*-KO PTCs was analyzed by Western blot. (B) Quantification of Rab11-FIP4 expression levels (normalized to actin, ACTB) from three independent experiments. $**P < 0.01$, unpaired Student's *t* test. (C) Immunofluorescence analysis of megalin (LRP2) localization in wild-type (WT), *CTNS*-KO, and GFP-Rab11-FIP4 expressing *CTNS*-KO PTCs. Arrowheads indicate plasma membrane localization. (D) Quantitative analysis of megalin localization at the plasma membrane. At least 50 cells per condition per experiment in a total of four independent experiments were analyzed. The symbols represent the mean of the percentage of cells presenting PM-associated megalin per field in each experiment. Between 5 and 12 fields were analyzed per condition per experiment. The error bars indicate the mean \pm SEM from four independent experiments. $***P < 0.001$. ns, not significant, one-way ANOVA, Tukey's multiple comparison test.

sequencing for confirmation (Retrogene). The wild-type and *Ctns*^{-/-} cells of murine fibroblasts and PTC cells were transfected using Lipofectamine 3000 (Thermo Fisher Scientific, 2103388) following the manufacturer's instructions and protein expression was confirmed by immunofluorescence analysis and Western blot. The transfection efficiency obtained using this procedure was $>90\%$ after 24 h. Expression vectors for the expression of DsRed-Rab11DN (12680; deposited by Dr Richard Pagano) and DsRED-Rab11a (12 679; deposited by Dr Richard Pagano) were purchased from Addgene.

Gel electrophoresis and immunoblotting

Cells were lysed in lysis buffer (20 mM Tris (pH 7.4), 150 mM NaCl, and 1% Triton X-100) in the presence of protease inhibitor (Roche Applied Science) and phosphatase inhibitors (Calbiochem). Protein concentration in diluted samples (0.01% Triton X-100) was measured using the colorimetric Bradford assay (Bio-Rad, 5000006). Gel electrophoresis was carried out using 4–12% gradient or 12% Bolt Bis-Tris Plus

gels (Life Technologies). Proteins were transferred onto 0.45- μ m nitrocellulose membrane, blocked in 5% blotto, and then the membranes were incubated overnight at 4 °C in the indicated primary antibodies, followed by incubation with HRP-conjugated secondary antibodies. The blots were developed using SuperSignal West Pico or Femto chemiluminescence substrate systems (Thermo Fisher Scientific). Proteins were visualized using Azure Biosystems C600 technology. All gels included 15 μ g of total protein per lane. The C600 utilizes CCD detectors that register signals in a range of $2^{16} = 65,536$ shades in grayscale, which indicates the instruments detect 4.82 orders of magnitude, a very wide dynamic range that allows for very strong and weak bands to be detected with a background contribution that tends to be negligible. Total loading was detected using Revert 700 Total Protein Stain (LiCor 926-11011), in addition to housekeeping genes, where indicated, to control for equal loading. Images are presented as acquired without any brightness or contrast adjustments. The following antibodies were used for immunoblotting in this study: rabbit anti-Rab11-FIP4 (LSC353582, Lifespan biosciences), anti-RAB7 (Cell Signaling Technology, 9367S), anti-

RAB11a (Cell Signaling Technology, 5589S), anti-actin (Santa Cruz Technologies, SC-7210 or SC-47778); anti-KDEL (Enzo Life Sciences, ADI-SPA-827), anti-LAMP1 (Santa Cruz Biotechnology, sc-19992); anti-LAMP2A (ThermoFisher Scientific, 51-2200), and rabbit anti-LC3B (2775, Cell Signaling Technology). All uncropped blots are included as supporting data (Supplementary data, Figure S3).

Immunofluorescence, immunohistochemistry, and confocal analysis

Murine fibroblast, CTNS-KD or wild-type 293FT and PTCs were seeded at 70% confluence in a four-chamber 35-mm glass-bottom dish (Cellvis, D35C4-20-1.5-N), then fixed with 4% paraformaldehyde for 8 min and blocked with 1% BSA in PBS, in the presence of 0.01% saponin, for 1 h. Samples were labeled with the indicated primary antibodies overnight at 4 °C in the presence of 0.01% saponin (Calbiochem, 558255) and 1% BSA. Samples were washed three times and subsequently incubated with the appropriate combinations of Alexa Fluor (488 or 594)-conjugated anti-rabbit, anti-rat, or anti-mouse secondary antibodies (Thermo Fisher Scientific, A-21206; A-21207; A-21208; A-21209; A-21202; A-21203, respectively). Nuclei were stained with 4,6-diamidino-2 phenylindole (DAPI) and samples were preserved in Fluoromount-G reagent (SouthernBiotech) and kept at 4 °C until analyzed. Samples were analyzed with a Zeiss LSM 880 laser-scanning confocal microscope attached to a Zeiss Observer Z1 microscope at 21 °C, using a 63× oil Plan Apo, 1.4-numerical aperture objective. Images were collected using ZEN-LSM software and processed using ImageJ software. The exposure time and gain were maintained throughout the experiment to comparatively analyze wild-type and *Ctns*^{-/-} cells. Analysis and quantification of protein colocalization were performed using ZEN-LSM software. Where indicated, images were acquired using enhanced resolution microscopy (Airyscan). To this end, 3D images were acquired using a Zeiss laser scanning confocal microscope (LSCM) 880 with Airyscan, using a 63× (1.4na) objective and the 32-channel GaAsP-PMT area detector. All Image stacks were acquired with Nyquist resolution parameters using a 0.159 μm step size, an optimal frame size of 2124 × 2124, and the same settings (laser power and detector gain) for all experiments. All Airyscan acquired images were processed using the ideal 3D default settings of the Airyscan processing module, which briefly, involves linear deconvolution and pixel reassignment for re-centering of the raw data. Images were further processed as maximum intensity projections (MIPs) in ZenDesk 3.0 (Zeiss) and analyzed using the Zen colocalization module. Briefly, ROIs were drawn around each individual cell, previously defined minimum thresholds were input (using secondary-only controls), two fluorescent channel signals for the indicated targets were selected and the calculation of pixel intensity spatial overlap correlation coefficients between two signals were automatically calculated using ZenDesk 3.0 (Zeiss). The following antibodies were used for immunofluorescence in this study: rabbit anti-RAB11-FIP4 (LSC353582, LSBio, Lifespan biosciences); anti-LAMP1 (Santa Cruz Biotechnology, sc-19992); anti-LAMP2A (Abcam, ab18528 or Thermo Fisher Scientific, 51-2200); rabbit

anti-GFP (Novus Biologicals, NB600-308SS) anti-KDEL (Enzo Life Sciences, ADI-SPA-827); and anti-LRP2 (Megalin) (Santa Cruz, sc-16476); anti-ATF4 (Cell Signaling Technology, 11815S); anti-CTNS, ABclonal A6893.

Starvation and treatment

Wild-type and *Ctns*^{-/-} MEFs were washed with serum-free DMEM (containing 1× amino acids). For macroautophagy studies, the media was aspirated, and fresh, serum-free DMEM, was added. The cells were then cultured at 37 °C incubator for 5 h, in the presence or absence of the lysosomal inhibitor bafilomycin A1 (100 nM) (LC laboratories, B-1080). Where indicated, MEFs were seeded onto 10 cm-diameter plates and cultured for 24 h until they reached a confluence of 70%. The media was replenished with fresh culture medium containing either 20 μM QX77 or 20 μM Genistein or vehicle (DMSO) and incubated for an additional 48 h before being harvested and processed for lysate preparation using RIPA buffer in the presence of protease inhibitors (Halt, Thermo Scientific). For Arf6 inhibition, where indicated, cells were treated with the selective Arf6 inhibitor NAV2729,²¹ at 10 μM for 24 h and subsequently transfected for the expression of Rab11-FIP4-GFP or mock-transfected, fixed, and analyzed by immunofluorescence.

Analysis of oxidative stress

The cell-permeable CellROX Deep Red probe (ThermoFisher, C10448) detects reactive oxygen species (ROS) in living cells. CellROX Deep Red dye is nonfluorescent in its reduced state but exhibits bright fluorescence when oxidized (excitation/emission maxima at 640/665 nm). CellROX Deep Red was added to WT, *ctns*^{-/-} and Rab11-FIP4-reconstituted *ctns*^{-/-} cells at a final concentration of 5 μM and the cells were then incubated for 30 min at 37 °C. Subsequently, the medium was removed, and the cells were washed three times with PBS. The resulting fluorescence was analyzed using a Zeiss LSM 880 laser-scanning confocal microscope attached to a Zeiss Observer Z1 microscope at 21 °C, using a 63× oil Plan Apo, 1.4-numerical aperture objective.

LC-MS/MS analysis of Rab11-FIP4 interactors

Proteomics analysis was performed at the Scripps Research Institute proteomics core facility. Briefly, 293FT cells expressing GFP-Rab11-FIP4 or GFP were lysed and samples were processed for immunoprecipitation using the GFP-nAb Magnetic agarose beads IP kit (Allele) following the manufacturer's instructions. Proteins were solubilized in 0.2% Rapigest (Waters Corporation) and reduced in 5 mM D, L-dithiothreitol (Sigma) for 30 min followed by alkylation with 15 mM iodoacetamide (Sigma) for 30 min in the dark. Proteins were digested with trypsin at 37 °C using a 1:30 (w/w) enzyme-to-substrate ratio. Peptides were analyzed by reverse-phase chromatography before mass spectrometry analysis exactly as we described before.⁴⁰

Statistical analysis

Data are presented as mean, and error bars correspond to standard errors of the means (SEMs) unless otherwise indicated. Statistical significance was determined using the unpaired Student's *t* test or ANOVA using GraphPad InStat (version 3) or Excel software, and graphs were made using GraphPad Prism (version 6) software. Further details of the analysis are described on the corresponding figure legend.

Authorship contribution

FR, experimentation, methodology, data analysis and manuscript editing; JLJ conceptualization, experimentation, methodology, data analysis and manuscript editing; EMS, experimentation, methodology; AS, DC, and MAK, experimentation; WBK, image acquisition, and analysis; EG and AMC, resources, manuscript editing; SC, manuscript editing and reagents, Methodology; SDC, designed strategy, conceptualization, data analysis, manuscript writing with input from JLJ.

Disclosure statement

No potential conflict of interest was reported by the authors.

Funding

Supported by fellowships from the Cystinosis Research Foundation to FR and EMS, by the National Institutes of Health grant numbers: R01HL088256, R01AR070837, R01DK110162, and P01HL152958 to S.D.C, and R01-DK090058 and R01-NS108965 for S.C. The Automated Zeiss LSM 980 Airyscan 2 Multiscale super-resolution confocal microscope was funded by an NIH S10 grant S10OD030417 to WBK.

ORCID

Sergio D. Catz  <http://orcid.org/0000-0002-1873-0277>

Data availability statement

The authors confirm that the data supporting the findings of this study are available within the article [and/or] its [supplementary materials](#). Additional data that support the findings of this study are openly available in figshare: dx.doi.org/10.6084/m9.figshare.27018577.

References

1. Town M, Jean G, Cherqui S, Attard M, Forestier L, Whitmore SA, Callen DF, Gribouval O, Broyer M, Bates GP, et al. A novel gene encoding an integral membrane protein is mutated in nephropathic cystinosis. *Nat Genet.* 1998;18:319–324. doi:10.1038/ng0498-319.
2. Kalatzis V, Cherqui S, Antignac C, Gasnier B. Cystinosin, the protein defective in cystinosis, is a H(+)-driven lysosomal cystine transporter. *EMBO J.* 2001;20:5940–5949. doi:10.1093/emboj/20.21.5940.
3. Napolitano G, Johnson JL, He J, Rocca CJ, Monfregola J, Pestonjamsk K, Cherqui S, Catz SD. Impairment of chaperone-mediated autophagy leads to selective lysosomal degradation defects in the lysosomal storage disease cystinosis. *EMBO Mol Med.* 2015;7:158–174. doi:10.15252/emmm.201404223.
4. Andrzejewska Z, Nevo N, Thomas L, Chhuon C, Bailleux A, Chauvet V, Courtoy PJ, Chol M, Guerrero IC, Antignac C. Cystinosin is a component of the vacuolar H⁺-ATPase-regulator complex controlling mammalian target of rapamycin complex 1 signaling. *J Am Soc Nephrol.* 2016;27:1678–1688. doi:10.1681/ASN.2014090937.
5. Rega LR, Polishchuk E, Montefusco S, Napolitano G, Tozzi G, Zhang J, Bellomo F, Taranta A, Pastore A, Polishchuk R, et al. Activation of the transcription factor EB rescues lysosomal abnormalities in cystinotic kidney cells. *Kidney Int.* 2016;89:862–873. doi:10.1016/j.kint.2015.12.045.
6. Cherqui S. Cysteamine therapy: a treatment for cystinosis, not a cure. *Kidney Int.* 2012;81:127–129. doi:10.1038/ki.2011.301.
7. Vaisbich M, Pache de Faria Guimaraes L, Shimizu M, Seguro A. Oxidative stress in cystinosis patients. *Nephron Extra.* 2011;1:73–77. doi:10.1159/000331445.
8. Zhang J, Johnson JL, He J, Napolitano G, Ramadass M, Rocca C, Kiosses WB, Bucci C, Xin Q, Gavathiotis E, et al. Cystinosin, the small GTPase Rab11, and the Rab7 effector RILP regulate intracellular trafficking of the chaperone-mediated autophagy receptor LAMP2A. *J Biol Chem.* 2017;292:10328–10346. doi:10.1074/jbc.M116.764076.
9. Johnson J, Napolitano G, Monfregola J, Rocca C, Cherqui S, Catz S. Upregulation of the Rab27a-dependent trafficking and secretory mechanisms improves lysosomal transport, alleviates endoplasmic reticulum stress, and reduces lysosome overload in cystinosis. *Mol Cell Biol.* 2013;33:2950–2962. doi:10.1128/MCB.00417-13.
10. Wallace DM, Lindsay AJ, Hendrick AG, McCaffrey MW. Rab11-FIP4 interacts with Rab11 in a GTP-dependent manner and its overexpression condenses the Rab11 positive compartment in HeLa cells. *Biochem Biophys Res Commun.* 2002;299:770–779. doi:10.1016/S0006-291X(02)02720-1.
11. Lindsay AJ, McCaffrey MW. The C2 domains of the class I Rab11 family of interacting proteins target recycling vesicles to the plasma membrane. *J Cell Sci.* 2004;117:4365–4375. doi:10.1242/jcs.01280.
12. Gorbea C, Pratt G, Ustrell V, Bell R, Sahasrabudhe S, Hughes RE, Rechsteiner M. A protein interaction network for Ecm29 links the 26S proteasome to molecular motors and endosomal components. *J Biol Chem.* 2010;285:31616–31633. doi:10.1074/jbc.M110.154120.
13. Muto A, Arai K, Watanabe S. Rab11-FIP4 is predominantly expressed in neural tissues and involved in proliferation as well as in differentiation during zebrafish retinal development. *Dev Biol.* 2006;292:90–102. doi:10.1016/j.ydbio.2005.12.050.
14. He Y, Ye M, Zhou L, Shan Y, Lu G, Zhou Y, Zhong J, Xue Z, Cai Z. High Rab11-FIP4 expression predicts poor prognosis and exhibits tumor promotion in pancreatic cancer. *Int J Oncol.* 2017;50:396–404. doi:10.3892/ijo.2016.3828.
15. Muto A, Aoki Y, Watanabe S. Mouse Rab11-FIP4 regulates proliferation and differentiation of retinal progenitors in a Rab11-independent manner. *Dev Dyn.* 2007;236:214–225. doi:10.1002/dvdy.21009.
16. Rahman F, Johnson JL, Zhang J, He J, Pestonjamsk K, Cherqui S, Catz SD. DYNC1L12 regulates localization of the chaperone-mediated autophagy receptor LAMP2A and improves cellular homeostasis in cystinosis. *Autophagy.* 2021;18:1108–1126. doi:10.1080/15548627.2021.1971937.
17. Zhang J, He J, Johnson JL, Rahman F, Gavathiotis E, Cuervo AM, Catz SD. Chaperone-mediated autophagy upregulation rescues megalin expression and localization in cystinotic proximal tubule cells. *Front Endocrinol (Lausanne).* 2019;10:21. doi:10.3389/fendo.2019.00021.
18. Moskot M, Montefusco S, Jakóbkiewicz-Banecka J, Mozolewski P, Węgrzyn A, Di Bernardo D, Węgrzyn G, Medina DL, Ballabio A, Gabig-Cimińska M. The phytoestrogen genistein modulates lysosomal metabolism and transcription factor EB (TFEB) activation. *J Biol Chem.* 2014;289:17054–17069. doi:10.1074/jbc.M114.555300.
19. Bourdenx M, Martín-Segura A, Scrivo A, Rodríguez-Navarro JA, Kaushik S, Tasset I, Diaz A, Storm NJ, Xin Q, Juste YR, et al. Chaperone-mediated autophagy prevents collapse of the neuronal metastable proteome. *Cell.* 2021;184:2696–2714.e25. doi:10.1016/j.cell.2021.03.048.

20. Fielding AB, Schonteich E, Matheson J, Wilson G, Yu X, Hickson GR, Srivastava S, Baldwin SA, Prekeris R, Gould GW. Rab11-FIP3 and FIP4 interact with Arf6 and the exocyst to control membrane traffic in cytokinesis. *EMBO J*. 2005;24:3389–3399. doi:10.1038/sj.emboj.7600803.
21. Finicle BT, Ramirez MU, Liu G, Selwan EM, McCracken AN, Yu J, Joo Y, Nguyen J, Ou K, Roy SG, et al. Sphingolipids inhibit endosomal recycling of nutrient transporters by inactivating Arf6. *J Cell Sci*. 2018;131. doi:10.1242/jcs.213314.
22. Gaide Chevronnay HP, Janssens V, Van Der Smissen P, N’Kuli F, Nevo N, Guiot Y, Levchenko E, Marbaix E, Pierreux CE, Cherqui S, et al. Time course of pathogenic and adaptation mechanisms in cystinotic mouse kidneys. *J Am Soc Nephrol*. 2014;25:1256–1269. doi:10.1681/ASN.2013060598.
23. Schafer JC, McRae RE, Manning EH, Lapierre LA, Goldenring JR. Rab11-FIP1a regulates early trafficking into the recycling endosomes. *Exp Cell Res*. 2016;340:259–273. doi:10.1016/j.yexcr.2016.01.003.
24. Horgan CP, McCaffrey MW. The dynamic Rab11-FIPs. *Biochem Soc Trans*. 2009;37:1032–1036. doi:10.1042/BST0371032.
25. Horgan CP, Hanscom SR, Jolly RS, Futter CE, McCaffrey MW. Rab11-FIP3 links the Rab11 GTPase and cytoplasmic dynein to mediate transport to the endosomal-recycling compartment. *J Cell Sci*. 2010;123:181–191. doi:10.1242/jcs.052670.
26. Wallace DM, Lindsay AJ, Hendrick AG, McCaffrey MW. The novel Rab11-FIP/RIP/RCP family of proteins displays extensive homo- and hetero-interacting abilities. *Biochem Biophys Res Commun*. 2002;292:909–915. doi:10.1006/bbrc.2002.6736.
27. Lindsay AJ, McCaffrey MW. Purification and functional properties of Rab11-FIP2. *Methods Enzymol*. 2005;403:491–499. doi:10.1016/S0076-6879(05)03043-0.
28. Horgan CP, Zurawski TH, McCaffrey MW. Purification and functional properties of Rab11-FIP3. *Methods Enzymol*. 2005;403:499–512. doi:10.1016/S0076-6879(05)03044-2.
29. Johnson JL, He J, Ramadass M, Pestonjamas K, Kiosses WB, Zhang J, Catz SD. Munc13-4 is a Rab11-binding protein that regulates Rab11-positive vesicle trafficking and docking at the plasma membrane. *J Biol Chem*. 2016;291:3423–3438. doi:10.1074/jbc.M115.705871.
30. Horgan CP, Hanscom SR, Jolly RS, Futter CE, McCaffrey MW. Rab11-FIP3 binds dynein light intermediate chain 2 and its overexpression fragments the Golgi complex. *Biochem Biophys Res Commun*. 2010;394:387–392. doi:10.1016/j.bbrc.2010.03.028.
31. Kumar R, Khan M, Francis V, Aguila A, Kulasekaran G, Banks E, McPherson PS. DENND6A links Arl8b to a Rab34/RILP/dynein complex, regulating lysosomal positioning and autophagy. *Nat Commun*. 2024;15:919. doi:10.1038/s41467-024-44957-1.
32. Longatti A, Lamb CA, Razi M, Yoshimura S, Barr FA, Tooze SA. TBC1D14 regulates autophagosome formation via Rab11- and ULK1-positive recycling endosomes. *J Cell Biol*. 2012;197:659–675. doi:10.1083/jcb.201111079.
33. Knævelsrud H, Søreng K, Raiborg C, Håberg K, Rasmuson F, Brech A, Liestøl K, Rusten TE, Stenmark H, Neufeld TP, et al. Membrane remodeling by the PX-BAR protein SNX18 promotes autophagosome formation. *J Cell Biol*. 2013;202:331–349. doi:10.1083/jcb.201205129.
34. Fader CM, Sánchez D, Furlán M, Colombo MI. Induction of autophagy promotes fusion of multivesicular bodies with autophagic vacuoles in K562 cells. *Traffic*. 2008;9:230–250. doi:10.1111/j.1600-0854.2007.00677.x.
35. Richards P, Didszun C, Campesan S, Simpson A, Horley B, Young KW, Glynn P, Cain K, Kyriacou CP, Giorgini F, et al. Dendritic spine loss and neurodegeneration is rescued by Rab11 in models of Huntington’s disease. *Cell Death Differ*. 2011;18:191–200. doi:10.1038/cdd.2010.127.
36. Voeltz GK, Sawyer EM, Hajnóczky G, Prinz WA. Making the connection: how membrane contact sites have changed our view of organelle biology. *Cell*. 2024;187:257–270. doi:10.1016/j.cell.2023.11.040.
37. Cherqui S, Courtoy PJ. The renal Fanconi syndrome in cystinosis: pathogenic insights and therapeutic perspectives. *Nat Rev Nephrol*. 2017;13:115–131. doi:10.1038/nrneph.2016.182.
38. Nevo N, Chol M, Bailleux A, Kalatzis V, Morisset L, Devuyt O, Gubler MC, Antignac C. Renal phenotype of the cystinosis mouse model is dependent upon genetic background. *Nephrol Dial Transplant*. 2010;25:1059–1066. doi:10.1093/ndt/gfp553.
39. Irizarry RA, Hobbs B, Collin F, Beazer-Barclay YD, Antonellis KJ, Scherf U, Speed TP. Exploration, normalization, and summaries of high density oligonucleotide array probe level data. *Biostatistics*. 2003;4:249–264. doi:10.1093/biostatistics/4.2.249.
40. Johnson JL, Meneses-Salas E, Ramadass M, Monfregola J, Rahman F, Carvalho Gontijo R, Kiosses WB, Pestonjamas K, Allen D, Zhang J, et al. Differential dysregulation of granule subsets in wash-deficient neutrophil leukocytes resulting in inflammation. *Nat Commun*. 2022;13:5529. doi:10.1038/s41467-022-33230-y.